https://doi.org/10.37434/tpwj2020.06.02

FEATURES OF STRUCTURE FORMATION AND PROPERTIES OF JOINTS OF S460M STEEL MADE BY PULSED-ARC WELDING

A.V. Zavdoveev[1], **V.D. Poznyakov**[1], **M. Rogante**[2], **S.L. Zhdanov**[1], **V.A. Kostin**[1] and **T.G. Soloveichuk**[1]
[1]E.O. Paton Electric Welding Institute of the NAS of Ukraine
11 Kazymyr Malevych Str., 03150, Kyiv, Ukraine. E-mail: office@paton.kiev.ua
[2]Rogante Engineering Office
62012 Civitanova Marche, Italy

The work is a study of the impact of pulsed-arc welding process on structure formation and properties of the metal of the weld and HAZ, compared to welding by a stationary arc. In the case of high-strength steel S450M, it is shown that pulsed-arc welding allows effective regulation of structure formation. Owing to a change of TWC, the weld and HAZ form a mixed structure that allows achieving high values of strength and brittle fracture resistance. 14 Ref., 1 Table, 6 Figures.

Keywords: pulsed-arc welding, high-strength steel, weld and HAZ metal, thermodeformational cycle, structure, welded joint properties

Pulsed arc welding (PAW) is characterized by periodically changed arc power [1−4], and due to its features, it allows solving complex technological problems in fabrication of unique structures, increasing the productivity of the welding processes, surfacing steels by corrosion-resistant alloys. In industrialized countries PAW is ever wider applied in fabrication of welded structures from structural steels of up to 500 MPa strength. This is attributable to the fact that at PAW the possibilities for controlling the processes of electrode metal melting and transfer in different positions are expanded, weld formation is improved, electrode metal mixing with base metal and HAZ dimensions are reduced [5−12]. This is exactly why the known welding equipment manufacturers in their activity give a lot of attention to development and manufacture of equipment for realization and widening of the possibilities of gas-shielded PAW. The publications provide much more limited coverage of the questions of the influence of PAW parameters on thermal processes, occurring in the metal of welded joint HAZ, as they affect the structure and mechanical properties of this metal, its cold cracking and brittle fracture resistance, etc. For successful application of PAW, during development of modern welding technologies, it became necessary to study the impact of the modes of this welding process on formation of the structure and properties of weld and HAZ metal, compared to welding by a stationary arc.

Investigation procedure. Thermomechanically strengthened S460M steel (C440 strength class), made to DSTU EN 10025-4:2007, was used in the work. Chemical composition of S460M steel is as follows, wt.%: 0.15 C; 0.23 Si; 1.3 Mn; 0.09 Cr; 0.019 Ni; 0.01 V; 0.05 Nb; 0.025 Al; 0.013 S and 0.017 P.

Used as the power source was inverter-type rectifier of ewm Phoenix Pulse 401 model (MULTIMATRIX Company), which ensures different pulse frequency in pulsed-arc welding. Digital oscillograph UTD2000CEX-II was used for determination of welding-technological characteristics of the power source, which allows conducting fixation of volt-ampere characteristic of the power source in a broad range. 75ShSM shunt with 150 μOhm resistance was used for recording the oscillograms. It allowed recording up to 500 A welding current. Here, the voltage drop on the shunt was equal to 75 mV.

Mechanized welding in shielding gases (Ar + 18 % CO_2) of joints of S460M steel 16 mm thick with V-shaped groove was performed by 1.2 mm G3Si1 solid wire. Root passes in welding this steel were made on a copper backing. Welding using a traditional process (stationary arc) was conducted in the following mode: I_w = 180–200 A, U_a = 26 V, v_w = 15–

A.V. Zavdoveev — https://orcid.org/0000-0003-2811-0765, V.D. Poznyakov — https://orcid.org/ 0000-0001-8581-3526,
M. Rogante — https://orcid.org/ 0000-0002-6846-0826, V.A. Kostin — https://orcid.org/0000-0002-2677-4667

18 m/h. The automated PAW mode was as follows: I_{av} = 220–240 A, U_a = 26–28 V, v_w = 14–21 m/h.

In this case

$$I_{av} = \frac{I_i t_i + I_p t_p}{t_i + t_p},$$

where I_i is the pulse current (450 A), I_p is the pause current (160 A), t_i and t_p is the duration of the pulse and pause, respectively.

Note that in addition to average PAW current, also effective PAW current is used, $I_{ef} = \sqrt{(1-\delta)I_p^2 + \delta I_i^2}$, where δ is the pulse duty cycle. So, taking the above PAW parameters into account, $I_{ef} \approx 300$ A that is almost by 25 % higher than I_{av}.

Metallographic investigations were performed using Neophot-32 light microscope, microhardness of individual structural components and integral hardness of the metal were measured in M-400 hardness meter of LECO Company at 100 g load (*HV*). Samples for metallographic studies were prepared by standard procedures with application of diamond pastes of different dispersity. Microstructures were revealed by chemical etching in 4 % alcohol solution of nitric acid.

Standard samples were prepared to conduct mechanical testing and determine the cold resistance of welded joints. Samples for testing for static (short-time) tension corresponded to type II to GOST 6996–96. Impact bend testing was performed to GOST 6996–66 (type IX) at the temperature of 20 and –40 °C. The conducted test results were used to assess the impact of the welding process on the change of the following HAZ metal characteristics: strength (σ_y and σ_t, MPa); ductility (δ_5 and ψ, %) and impact toughness (*KCV*, J/cm^2).

Metal ability to resist brittle fracture was determined using fracture mechanics approaches. In keeping with fracture mechanics procedure, the critical coefficient of stress intensity K_{1C} is used for evaluation of metal sensitivity to stress concentration under the conditions of plane deformation at static loading (more often by bending). At increase of K_{1C}, metal sensitivity to stress concentration decreases. The second criterion of fracture mechanics — critical crack opening δ_c is a deformation criterion, and it is used for evaluation of metal resistance to crack initiation. It is applied for assessment of brittle fracture resistance of the metal under the conditions of high plastic deformation, when the crack reaches critical dimensions, δ_c value in its tip and starts propagating quickly, using the energy released at its further growth.

Values of K_{1C} and δ_c criteria were determined by standard procedures.

The values of critical stress intensity factor K_{1C} were determined by the following formula:

$$K_{1C} = \frac{PLY}{t\sqrt{b^3}}, \quad (1.1)$$

where P is the critical load, at which the sample breaks; L is the distance between the supports; t is the sample thickness; b is the sample width; Y is the sample form factor.

Critical crack opening δ_c was determined by the following formula:

$$\delta_c = \frac{4K_{1C}^2}{\pi\sigma_y E}, \quad (1.2)$$

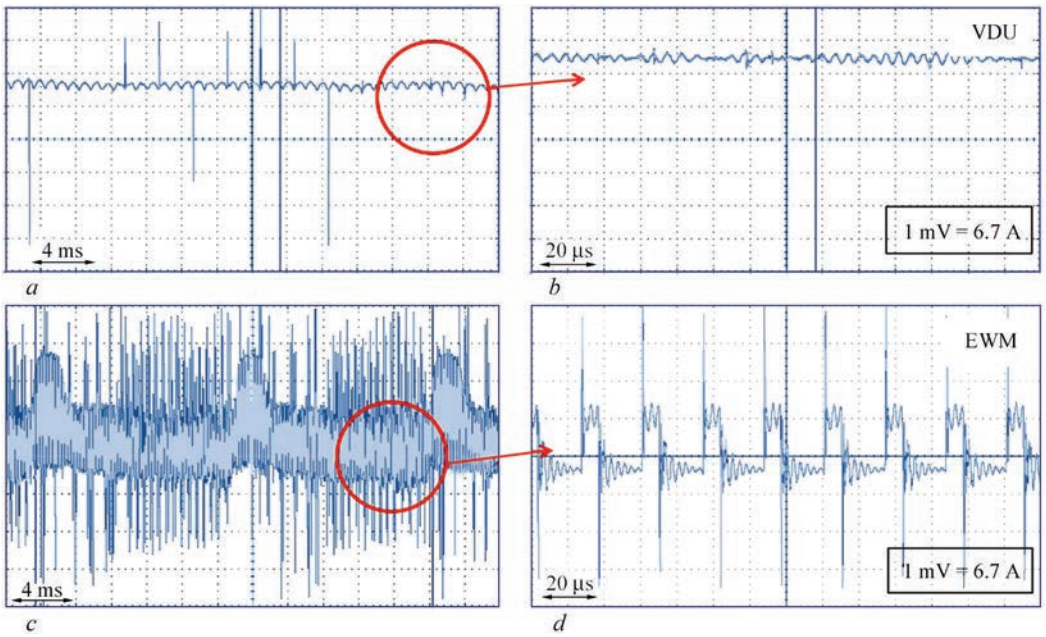

Figure 1. Oscillograms of welding current for power sources of diode and inverter types (for description see the text)

where E is the Young's modulus, which is equal to 200 GPa for steel.

The values of critical stress intensity factor K_{1C} and critical crack opening δ_c were determined on samples of a rectangular cross-section of 10×20×90 mm size with 7 mm long notch and 3 mm long fatigue crack. These samples were tested by three-point bending in the temperature range from 20 to −40 °C.

Research results and their discussion. *Welding-technological characteristics.* Power source ewm Phoenix Pulse 401 is of inverter type. In this connection, comparison of volt-ampere characteristics with VDU500 power source fitted with a rectifier was conducted. Results given in Figure 1 show that the above current sources differ essentially by the characteristics of welding current change. It is established that the stationary welding mode, using VDU power source is characterized by direct current with small oscillations. Current value in the oscillogram corresponds to 120 A. For ewm Phoenix Pulse 401 power source fitted with inverter rectifier, the dependence of the change of welding current is fundamentally different. At small scan waveform ($\tau \sim$ ms) a wide band of dense pulses of rather large amplitude is observed (Figure 1, *c*). In order to reveal the features of ampere characteristic, the scan waveform scale was increased to microseconds (Figure 1, *d*). Under such conditions, the peculiarities of welding current change are manifested, which are of a pulsed nature. Average welding current at pulsed-arc process was selected for comparison with the current of stationary arc welding.

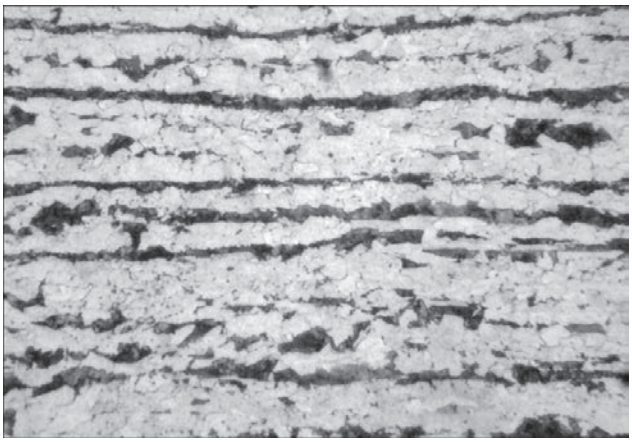

Figure 2. Microstructure (×500) of S460M steel

Base metal structure and properties. Owing to performance of thermomechanical rolling in the temperature range of 900–700 °C with controlled cooling, a ferrite-pearlite banded structure with hardness *HV*195 forms in S460M steel (Figure 2). Grain size number corresponds to No.10 to GOST 5639−82, and band point — to number 5 by scale 3 to GOST 5640−68.

Such a microstructure of S460M steel of the above-given composition ensures the following level of mechanical properties: yield limit $\sigma_{0.2}$ = 452 MPa, ultimate strength σ_t = 581 MPa, relative elongation δ_5 = 26 %; reduction in area ψ = 58 %.

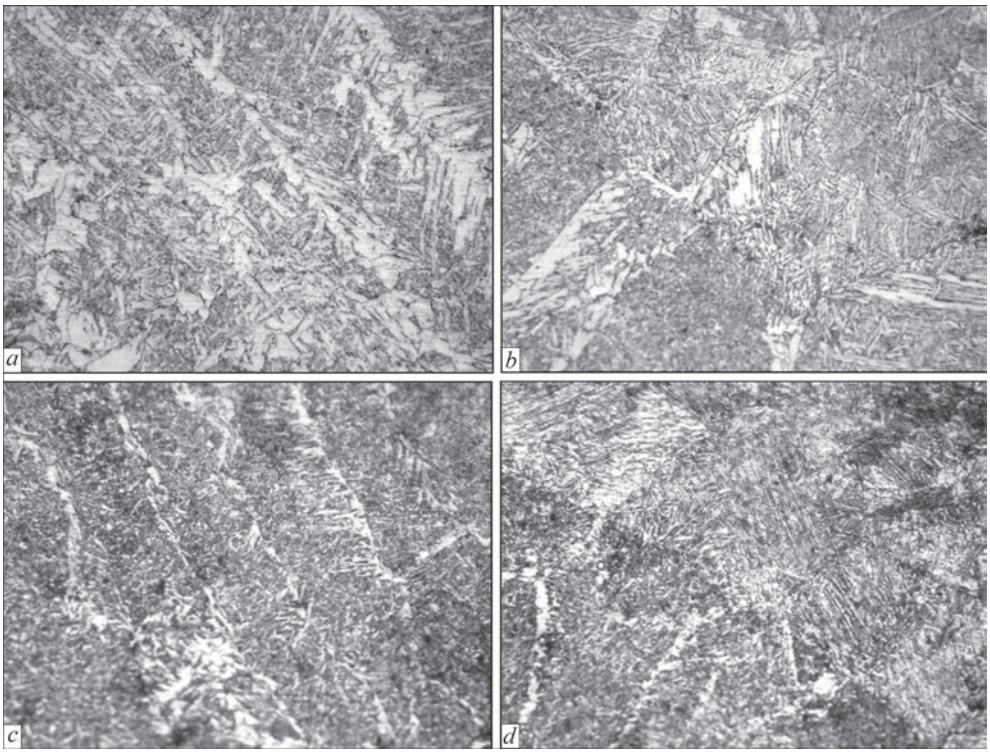

Figure 3. Microstructure (×500) of the metal of weld (*a*, *c*) and HAZ (*b*, *d*) of S460M steel, made by the traditional arc (*a*, *b*) and pulsed-arc welding

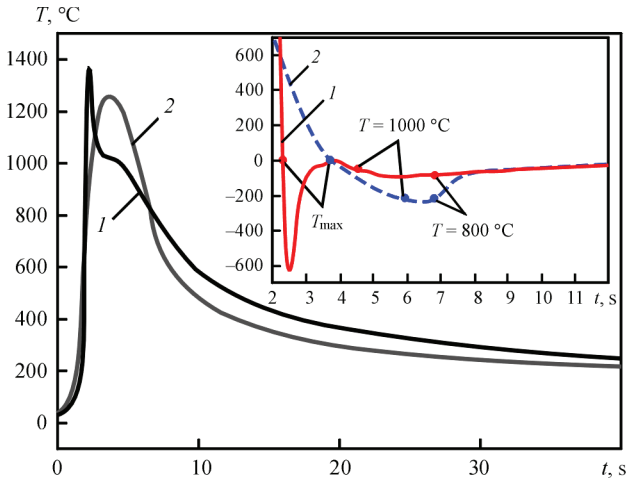

Figure 4. Thermal welding cycles for PAW (*1*) and AW (*2*)

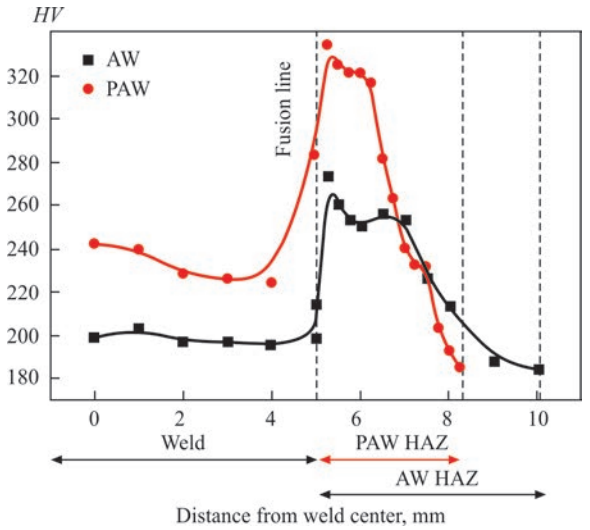

Figure 5. Hardness of welded joints of S460M steel

Metallographic studies of the structure (Figure 3) of welded joints of S460M steel showed that in welding by a stationary arc, the weld forms a predominantly ferrite structure of different modifications (polygonal, polyhedral, coarse acicular). Vickers hardness of such a structure is within 1950 to 2030 MPa. The microstructure of a coarse-grain zone of the HAZ consists of a mixture of upper and lower bainite. Vickers hardness of this HAZ zone reaches 2730 MPa. In the fine-grain zone of HAZ metal predominantly the structure of upper bainite is observed. The hardness of this HAZ zone decreases to 2600 MPa. In incomplete recrystallization zone of the HAZ, ferrite and pearlite form near the bainite zone that essentially lowers the hardness to 2130–2260 MPa.

At PAW the weld metal microstructure differs essentially from that of the metal of a weld, made by arc welding, namely: acicular ferrite needles are refined significantly (to 1–3 μm) and the amount of polyhedral ferrite decreases (to 5–10 %); polygonal ferrite precipitates, located on the boundaries of primary austenite grains, are narrowed considerably (to 3–10 μm). Such microstructural changes lead to increase of weld hardness to 2420 MPa. In the coarse grain zone of the HAZ metal a predominantly bainite structure with a small fraction of martensite (up to 3–5 %) is observed. The hardness of this HAZ region rises to 3250–3340 MPa, respectively. The structure of fine grain zone of the HAZ metal consists of a mixture of upper and lower bainite (2650–2810 MPa). Pearlite and ferrite are found in incomplete recrystallization zone of the HAZ that essentially lower the Vickers hardness of the metal to 2320–2400 MPa.

Such microstructural differences are due to the features of running of thermal welding cycles (TWC) at PAW (Figure 4), namely, metal cooling rate in the HAZ zones, which are heated to temperatures of 1000 °C and more, is lower than that during welding by a stationary arc. Due to that martensite components appear in the structure. In the HAZ, where the metal is heated up to temperatures below 1000 °C, the metal cooling rate is lower than in welding by a stationary arc. This promotes running of the diffusion processes during structural transformations, and, consequently, formation of a mixed bainite-martensite structure.

As noted by the authors of work [13], TWC has a key role at weld metal hardening, as it influences the refinement of the structural components. At PAW arc interruption occurs, which causes thermal «shock» (metal deposition is interrupted) that leads to increase of solidification centers. As a result, the structure is refined and strength characteristics are increased.

Hardness studies (Figure 5) of welded joints revealed that at PAW its level in the weld metal is 20 % higher than metal hardness in a weld made by the arc process. This is due to formation of a fine structure. In

Mechanical properties of 3460M steel welded joints at different welding methods

Weld length	Welding process	σ_y, MPa	σ_t, MPa	δ, %	ψ, %	KCV_{+20}, J/cm²	KCV_{-40}, J/cm²
Weld	AW	477	586	28	73	215	100
	PAW	570	667	24	68	212	111
HAZ	AW	632*	763*	–	–	149	150
	PAW	778*	940*	–	–	137	122
BM		452	581	26	60	111	95

*Calculated values [14]: σ_t — $HV0.31$, σ_y — $HV0.25$.

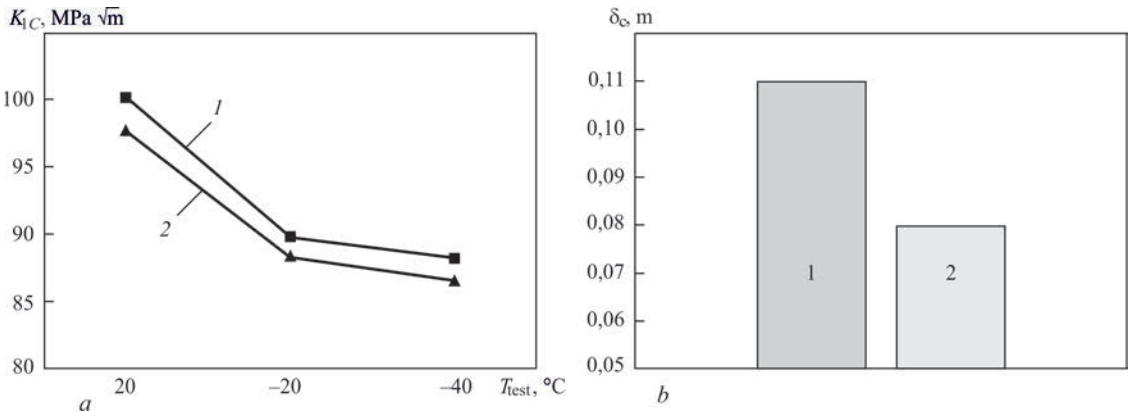

Figure 6. K_{1C} (*a*) and δ_c (*b*) for PAW: *1* — weld; *2* — HAZ

the HAZ the hardness values at PAW are also higher than at AW, but, despite that, they do not exceed the values of *HV*350, i.e. in such metal cold cracking will be improbable. It should be noted that at PAW, HAZ metal hardness decreases to initial metal level faster.

Mechanical properties of welded joints are given in the Table. One can see from the given data that under PAW conditions, higher strength values are achieved at preservation of impact toughness values on the level of the requirements of EN 10025-2 (SBC V2.6.-198:2014), $KCV_{-40} \geq 25$ J/cm^2. The values of brittle fracture resistance of welded joints made by PAW, despite the high hardness values, are at a rather high level (Figure 6) that is due to formation of a fine structure.

Thus, PAW allows effective regulation of structure formation in welded joints of high-strength steels. Under the conditions of approximately the same input energies, the effective welding current at PAW is by 25 % higher than in stationary arc welding. This allows increasing the penetration depth. The features of a pulsed change of welding current essentially change the TWC nature, and, consequently, the HAZ structure. Formation of a mixed structure in the HAZ allows achieving high values of strength and brittle fracture resistance.

Conclusions

Analysis of experimental data showed that at PAW, owing to a change of TWC (increase of the cooling rate in the temperature range > 1000 °C), a refined structure forms in the weld, compared to AW, and quenching structures form in the HAZ. Here, the HAZ metal cooling rate in the temperature range of 600–500 °C decreases practically 1. 5 times, that allows reducing the HAZ width by 40 %. As a result of testing, it was established that the metal of the welds and HAZ of welded joints of S460M steel, made by PAW, has sufficiently high brittle fracture resistance in the studied temperature range, and 20 % higher strength values.

1. Palani, P.K., Murugan, N. (2006) Selection of parameters of pulsed current gas metal arc welding. *J. Materials Proc. Technology*, **172**, 1–10.
2. Tong, H., Ueyama, T. et al. (2001) Quality and productivity improvement in aluminium alloy thin sheet welding using alternating current pulsed metal inert gas welding system. *Sci. Technol. Weld. Join*., 6(**4**), 203–208.
3. Needham, J.C., Carter, A.W. (1965) Material transfer characteristics with pulsed current. *Brit. Weld. J.*, **5**, 229–241.
4. Poznyakov, V.D., Zavdoveev, A.V., Gajvoronsky, A.A. et al. (2018) Effect of pulsed-arc welding modes on the change of weld metal and HAZ parameters of welded joints produced with Sv-08Kh20N9G7T wire. *The Paton Welding J*., **9**, 7−12.
5. Rajasekaran, S. (1999) Weld bead characteristics in pulsed GMA welding of Al–Mg alloys. *Weld. J.*, 78(**12**), 397–407.
6. Murray, P.E. (2002) Selecting parameters for GMAW using dimensional analysis. *Ibid.*, 81(**7**), 125–131.
7. Amin, M., Ahmed, N. (1987) Synergic control in MIG welding 2–power current controllers for steady dc open arc operation. *Met. Construct*., June, 331–340.
8. Amin, M. (1983) Pulse current parameters for arc stability and controlled metal transfer in arc welding. *Ibid.*, May, 272–377.
9. Lambert, J.A. (1989) Assessment of the pulsed GMA technique for tube attachment welding. *Weld. J.* 68 (2), 35–43.
10. Essers, W.G. Van Gompal (1984) Arc control with pulsed GMA welding. *Ibid.*, 6(**6**), 26–32.
11. Amin, M. (1981) Synergetic pulse MIG welding. *Metal Construction*, **6**, 349–353.
12. Dorn, L., Devakumaran, K., Hofmann, F. (2009) Pulsed current gas metal arc welding under different shielding and pulse parameters. Pt 2: Behaviour of metal transfer. *ISIJ Intern*., 49(**2**), 261–269.
13. Devakumaran, K., Ghosh, P.K. (2010) Thermal characteristics of weld and HAZ during pulse current gas metal arc weld bead deposition on HSLA steel plate. *Materials and Manufacturing Processes*, 25(**7**), 616–630, DOI:10.1080/10426910903229347.
14. Chukin, M.V., Poletskov, P.P., Gushchina, M.S., Berezhnaya, G.A. (2016) Determination of mechanical properties of high-strength steels by hardness. *Obrabotka Sploshnykh i Sloistykh Materialov*, 44(**1**), 28–35 [in Russian].

Received 06.02.2020